

## Research Article

# Fire Resistance Investigation of Simple Supported RC Beams with Varying Reinforcement Configurations

Yamin Song <sup>1</sup>, Chuanguo Fu,<sup>2</sup> Shuting Liang <sup>1</sup>, Ankang Yin,<sup>2</sup> and Longji Dang<sup>1</sup>

<sup>1</sup>School of Civil Engineering, Southeast University, Nanjing, China

<sup>2</sup>School of Civil Engineering, Shandong Jianzhu University, Jinan, China

Correspondence should be addressed to Yamin Song; sym511@126.com

Received 9 January 2019; Revised 18 March 2019; Accepted 14 April 2019; Published 2 May 2019

Academic Editor: Ignacio Paya-Zaforteza

Copyright © 2019 Yamin Song et al. This is an open access article distributed under the Creative Commons Attribution License, which permits unrestricted use, distribution, and reproduction in any medium, provided the original work is properly cited.

To investigate fire-resistance behaviors of simple supported reinforced concrete (RC) beams with three faces exposed to fire, six full-scale specimens were designed in accordance with the principle of “strong bending and weak shearing.” One beam was treated as the control case of room temperature while the other five beams were exposed to high temperature. Parameters related to shear capacity were discussed, such as longitudinal reinforcement ratio and stirrup ratio. The experimental results show that brittle shear failure under room temperature may transfer to shear-bend failure at high temperature due to thermal expansion and strength degradation of concrete and steel. The greater the longitudinal reinforcement ratio, the longer the failure time of specimens. It indicates that the pinning action of longitudinal reinforcement can significantly improve the shear capacity of beams under high temperature. In addition, the configuration of stirrup reinforcement can effectively reduce the brittle change of vertical deflection when the beam enters the failure stage.

## 1. Introduction

Reinforced concrete (RC) beams present thermal deformations under fire. The mechanical properties of steel and concrete degrade at high temperature due to changes of internal physical parameters, thus the fire-damaged RC members may not be able to perform expectedly. Therefore, it is of great significance to strengthen the investigation on the fire resistance of RC members or the entire RC structure. Previous research focused on studying the flexural capacity of RC beams under fire, with little attention on shear capacity.

The shear performance of RC members under fire is usually studied based on experiments and finite element (FE) analyses. Lu et al. [1] investigated the response of RC beams through fire resistance experiments on twelve simple supported RC beams. The main parameters were service loads, elevated temperature curves, and concrete cover. Fu et al. [2] tested two full-scale prestressed steel reinforced concrete (PSRC) simply supported beams under thermodynamics coupling, investigating the distribution of temperature field, vertical deformation characteristics, and

bearing performance deterioration process. Khan et al. [3] conducted shear tests on one hundred eleven RC beams to assess the influence of cyclic thermal loading on the shear strength of reinforced concrete (RC) beam specimens. Investigated factors included reinforcements, thermal cycles, and peak temperature. Faris et al. [4] carried out fire resistance tests on ninety-nine high and normal strength concrete elements subjected to elevated temperatures, with a focus on explosive spalling. Ahmed and Kodur [5] tested four RC beams strengthened with carbon fiber-reinforced polymer (CFRP). Dwaikat and Kodur [6] presented results from fire resistance experiments on six RC beams to illustrate the comparative performance of high-strength concrete (HSC) and normal-strength concrete (NSC) beams exposed to fire. Ryu et al. [7] designed an experiment on twelve RC beams with different loads and different cross sections exposed to high temperatures following the ISO 834 standard time temperature. The fire-damaged beams were then loaded with four-point loading to obtain its residual strength. Wu et al. [8] investigated the effect of cracks on temperature distributions of ten concrete members subjected to postearthquake fire. Christopher and Elin [9] presented

a procedure of conducting reliability analysis of prestressed concrete beams subjected to fire load. Kang et al. [10] investigated the effect of thickness and moisture on temperature distributions of reinforced concrete walls under fire conditions. Gabriela et al. [11] conducted a series of fire resistance tests on axially and/or rotationally restrained RC beams under flexural bending to study the failure modes and fire resistance of the RC beams and compared the behavior in restrained and unrestrained conditions. Fu et al. [12] designed eight full-scale reinforced concrete beams to investigate shear capacity of RC beams under thermodynamic coupling. Many researchers used finite element software to study the fire resistance performance of members under high temperature [13–21]. As shown, there is little research on the fire resistance of RC members exposed to fire.

Therefore, six RC beams are designed in this study according to the “strong bending and weak shearing” principle to test their resistance performance against fire and load. One of them is used as the reference to carry out four-point-bending tests at ambient temperature in determining the ultimate load bearing capacity. The other five beams are used to carry out the fire resistance tests with three faces exposed to high temperature following the standard ISO 834 fire curve [22]. That is, they are first subjected to impact loadings and then exposed to fire with a constant load. The effectiveness of longitudinal reinforcement ratio and stirrup ratio on fire resistance of RC beams are evaluated in particular.

## 2. Experimental Program

To assess the fire resistance of simple supported RC beams with varying reinforcement configurations, five RC beams were tested under fire. For comparison purposes, an additional RC beam was also tested at ambient temperature. The test variables included longitudinal reinforcement ratio ( $\rho$ ) and stirrup ratio ( $\rho_{sv}$ ).

**2.1. Specimens Details.** Six full-scale RC beam specimens of 250 mm (width)  $\times$  400 mm (depth)  $\times$  4000 mm (length) were fabricated in the Structural Engineering Laboratory of Shandong Jianzhu University, as shown in Figure 1 and Table 1. The specimens B1, B2, B5, and B6 were longitudinally reinforced with 4 C 25 at the bottom sides, corresponding to a  $\rho$  of 1.96%, while the bottom longitudinal reinforcements of specimen B3 were 2 C 25 and 2 C 20, corresponding to a  $\rho$  of 1.61%. The longitudinal reinforcement ratio of B4 was 1.47%. The shear span ratio  $\lambda$  of all the beams was 2.1, and the load ratio in the fire resistance test was  $0.4 P_u$ , where  $P_u$  was the ultimate load bearing capacity at ambient temperature. The cover thickness of the longitudinal bars was 25 mm.

**2.2. Material Properties.** All beams were fabricated with commercial concrete, using ordinary Portland cement from Jinfeng City. The mix proportions and materials used in the concrete mix design are shown in Table 2. Three concrete cubes (150 mm  $\times$  150 mm  $\times$  150 mm) were cast and tested to obtain the material properties, and the tested average

compressive strength was 31.6 MPa. The steel bar samples were taken from each type of rebars for tensile tests to obtain the yield  $f_y$  and the ultimate  $f_u$  strengths. The tested material properties are given in Table 3.

**2.3. Test Setup and Instrumentation.** The horizontal furnace chamber for the fire tests has a floor area of 9000 mm (length)  $\times$  4500 mm (width) and a height of 1500 mm in the Fire Laboratory of Shandong Jianzhu University, as shown in Figure 2(a). According to the experimental design, the fire tests were conducted in the furnace chamber, as shown in Figure 2(b). To measure the vertical displacement under fire by a data logger, four linear variable differential transducers (LVDT) were set up at the midspan, support, and two load points to measure the vertical deformations, as shown in Figure 2(c). The load was kept constant during the fire test and the general arrangement of the test setup is shown in Figure 2(d). The test temperature was controlled under the ISO 834 standard fire curve with three faces. Four thermocouples were used for measuring the temperature in the furnace, and the average for the four measured temperatures was used as the representative temperature of the furnace. The temperatures in the cross section were measured by thermocouples, as shown in Figure 3.

**2.4. Failure Criterion.** Two failure criteria were checked during the fire resistance tests, a deformation and a resistance criterion. According to Chinese Standard (GB/T9978.1-2008) [23], the deformation criterion was defined. When either of the indices exceeds the deformation (equation (1)) and deformation rate (equation (2)), it was considered to have failed:

$$\text{deformation: } D = \frac{L^2}{400d} \text{ mm}, \quad (1)$$

$$\text{deformation rate: } \frac{dD}{dt} = \frac{L^2}{9000d} \text{ mm/min}, \quad (2)$$

where  $L$  is the net span of the specimen (mm) and  $d$  is the height between the compression point and the tensile point on the cross section of the specimen (mm).

The failure criterion in terms of resistance is assumed when the beam experiences brittle failure and momentary loses its bearing capacity.

The minimum failure times based on these limit states is considered to be the fire resistance of the beam.

## 3. Results and Discussion of the Static Load Test

To determine their ultimate load bearing capacity, the experimental program comprised firstly four-point-bending tests on reference beams at ambient temperature. These tests were carried out for having reference values to compare with the ones calculated according to Chinese Standard [24] requirement and define the loads to be applied in the tests at high temperature. Considering all the specimens experienced a similar damage process, the test phenomenon will not be described in detail one by one. Only the failure mode of specimen B1 is illustrated in Figure 4.

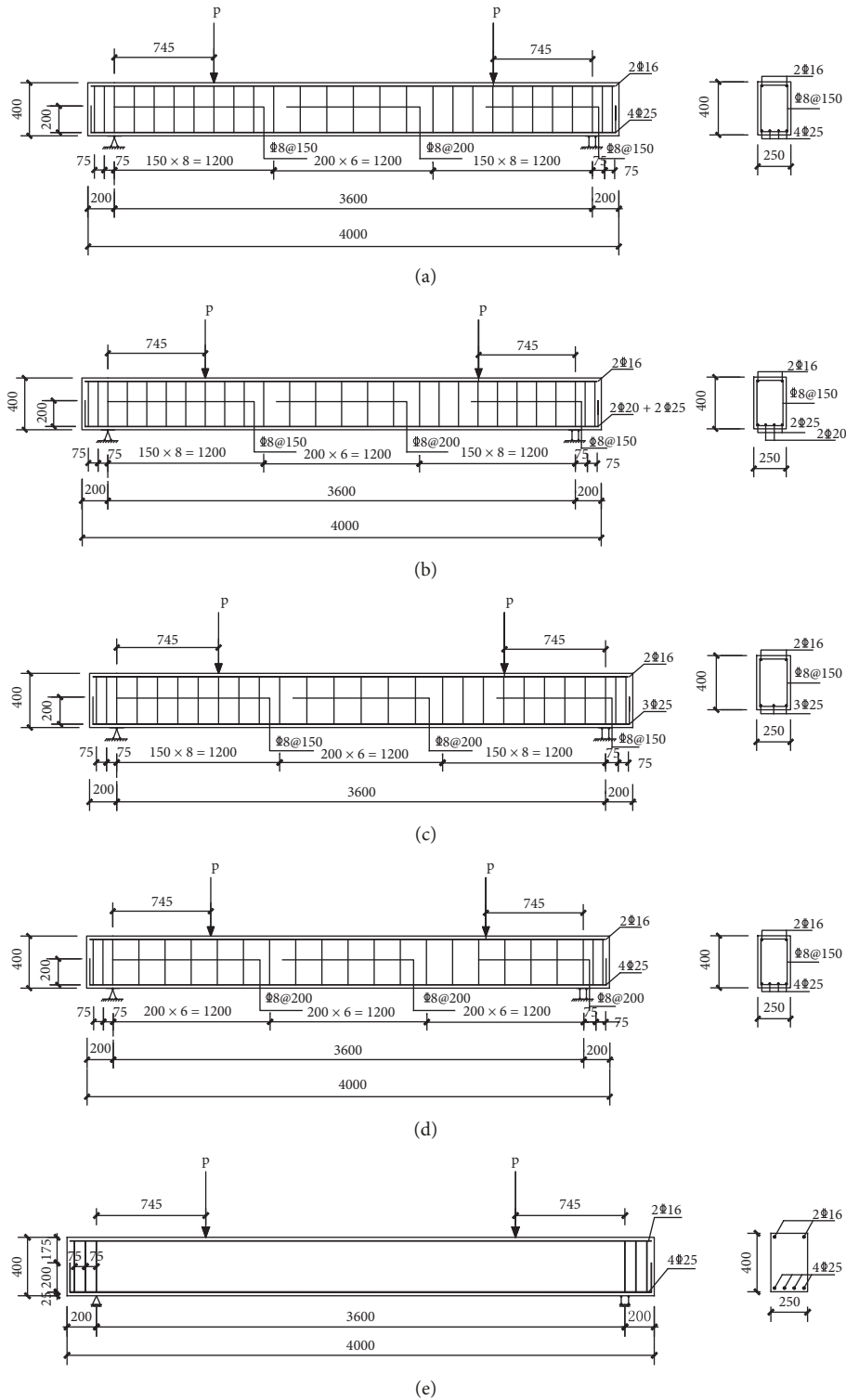


FIGURE 1: Dimensions and reinforcement details (dimensions in mm): (a) B1, B2, (b) B3, (c) B4, (d) B5, and (e) B6.

#### 4. Results and Discussion of the Fire Tests

The data generated from the above fire tests can be used to study the overall performance of RC beams under fire conditions. The thermal and structural responses of beams are compared to evaluate the effects of longitudinal reinforcement ratio and stirrup ratio. After the fire resistance

tests, the specimens were cooled naturally by air cooling via convection.

**4.1. Thermal Response.** Strict temperature control according to ISO834 could not be conducted due to the limitation of furnace equipment. For instance, the difference in the

TABLE 1: Specimens parameters.

Specimen	Cross section (mm)	$\rho_{sv}$ (%)	Stirrup legs	$\rho$ (%)	$\lambda$	Load ratio
B1	250 × 400	0.27	2	1.96	2.1	—
B2	250 × 400	0.27	2	1.96	2.1	0.4P <sub>u</sub>
B3	250 × 400	0.27	2	1.61	2.1	0.4P <sub>u</sub>
B4	250 × 400	0.27	2	1.47	2.1	0.4P <sub>u</sub>
B5	250 × 400	0.20	2	1.96	2.1	0.4P <sub>u</sub>
B6	250 × 400	0.00	/	1.96	2.1	0.4P <sub>u</sub>

TABLE 2: Mix proportions of the concrete.

Material	Specification	Unit weight (kg/m <sup>3</sup> )	Mixture ratio
Cement	P.O 42.5	206	1.00
Fine aggregates	Medium sands	752	2.46
Coarse aggregates	Particle sizes (5–25 mm)	1042	3.41
Water	Purified water	180	0.59
Admixtures	JX-1	8.08	0.03
Fly ash	Grade I	97.77	0.32

Cement: P.O. 42.5 (Chinese cement grading system) ordinary Portland cement from Jinfeng city. Fly ash: Grade I (Chinese fly ash grading system) fly ash of Jiangsu Huawang brand. Additives: JX-1 produced by Xingbang Co., Jining city.

TABLE 3: Mechanical properties of reinforcement.

Sample	Diameter, $d$ (mm)	Yield strength, $f_y$ (MPa)	Ultimate strength, $f_u$ (MPa)
C 8	8	380	600
C 16	16	445	580
C 20	20	413	548
C 25	25	451	593

performance of gas burners and the exhaust system caused fluctuation in the furnace temperature. Therefore, stable fire of gas was maintained during the whole fire test, and the data of furnace temperature were obtained by the thermocouples, as shown in Figure 5. It was evident that the furnace temperature was lower than the ISO 834 standard temperature curve. During the fire resistance tests, Figure 6 shows the measured temperature through partial thermocouples of the five specimens with the fire exposure time. The temperatures collected by thermocouples decreased with the increase of embedded depth at the same cross section.

**4.2. Measured Vertical Deflection.** Table 4 illustrates the failure time under fire of each specimen. Figure 7 shows the vertical deflection of the maximum deflection measuring point as a function of fire exposure time for beams with different parameters. The deflections started to increase slowly up to a certain point and then increase sharply. Through analysis of these curves, the following conclusions can be obtained:

- (1) As shown in Figure 7(a) and Table 4, the vertical deflection of three specimens B2, B3, and B4

increased gently before about 140 min, and then specimen B4 increased fast and reached the fire resistance at 171 min. The vertical deformation rate of specimen B3 was between B4 and B2, reaching the failure time at 180 min. Specimen B2 with the largest longitudinal reinforcement ratio had the smallest vertical deflection and reaches the fire resistance at 192 min. Therefore, the greater the longitudinal reinforcement ratio, the longer the failure time of the specimen, which indicates that the pinning action of the longitudinal reinforcement can significantly improve the shear capacity of the specimen at high temperature.

- (2) Due to the stirrup ratio, the vertical deflections of specimens B2 and B5 were slower than that of specimen B6 when they reached the fire resistance. The stirrup ratio has no obvious regular influence on the fire resistance of simple supported RC beam under fire, but the configuration of the stirrup can effectively reduce the brittle change of the vertical displacement when the beam enters the failure stage. However, the beam B6 achieved a slow rise in midspan deflection, as shown in Figure 7(b). This is due to the loading process using 10 t manual jacks, and the applied loading were monitored during the whole fire tests, but the manual jacks were unstable. It could be noted that beam B6, without internal stirrups, achieved a remarkably higher fire resistance. This is because B6 carried out the fire resistance test with the other beams without internal stirrups, and the furnace temperature is not the same. In addition, the beam B6 produces longitudinal spalling, causing the increasing of the midspan deflection at a certain degree. However, one of the failure criteria is the deformation during the fire resistance tests, which extends the failure time of beam B6.

**4.3. Failure Modes.** Figure 8 summarizes the failure modes of all the specimens at fire resistance tests. Many vertical cracks appeared in middle pure flexure section of specimen B2, while there were many diagonal cracks in the shear-bending section, and the maximum width of the diagonal cracks basically reached 1 mm, as shown in Figure 8(a). There were long penetrating diagonal cracks through the applied load point. Therefore, specimen B2 had the characteristic of shear-bend failure at high temperature.

As can be seen in Figure 8(b), flexural and shear cracks appeared in the shear-bend section of specimen B3, in which the maximum width of the diagonal crack was up to 2 mm, and more cracks were derived, while the vertical cracks were not obvious in the pure flexure section. Finally, the failure mode of specimen B3 exhibited shear-bend failure at high temperature.

More vertical cracks with the width of mostly less than 1 mm appeared in the pure flexure section of specimen B4, while many main diagonal cracks with the maximum width of 2 mm emerged in the shear-bending section. Observing

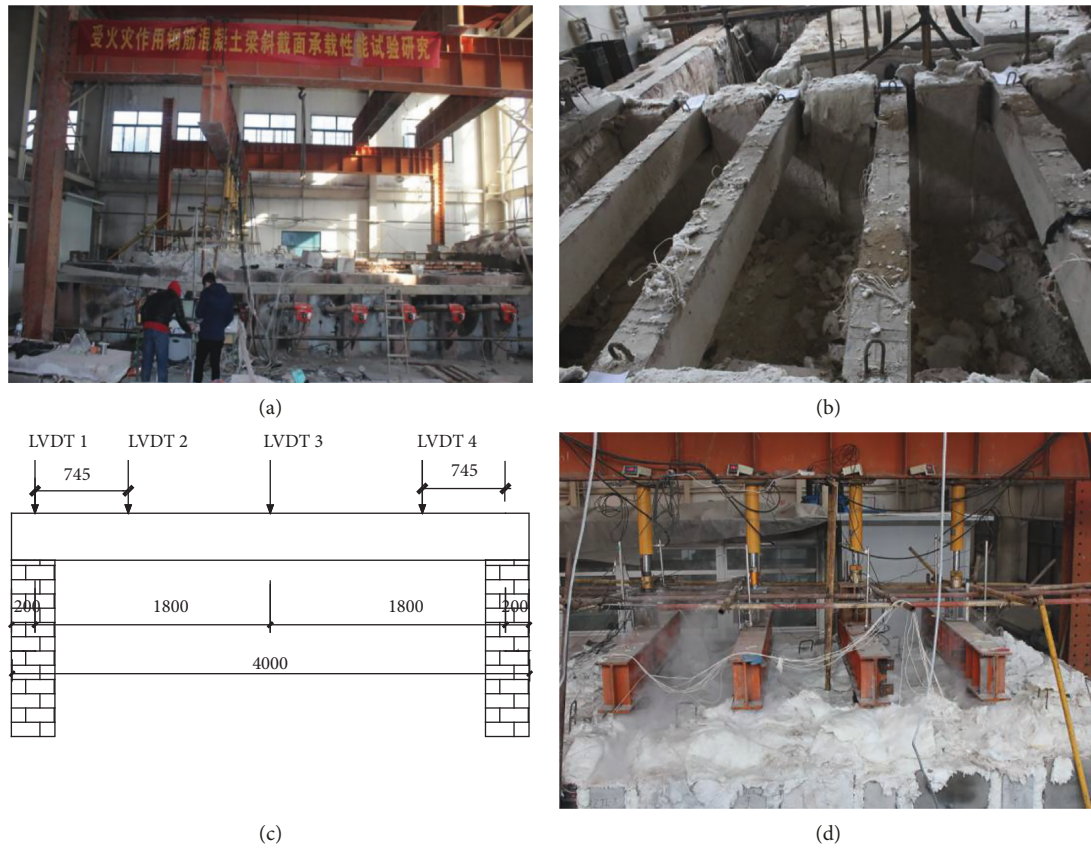


FIGURE 2: Test setup for the fire resistance tests (dimensions in mm). (a) The furnace chamber. (b) Specimens arrangement in the fire chamber. (c) LVDTs layout. (d) Load site of the test specimens.

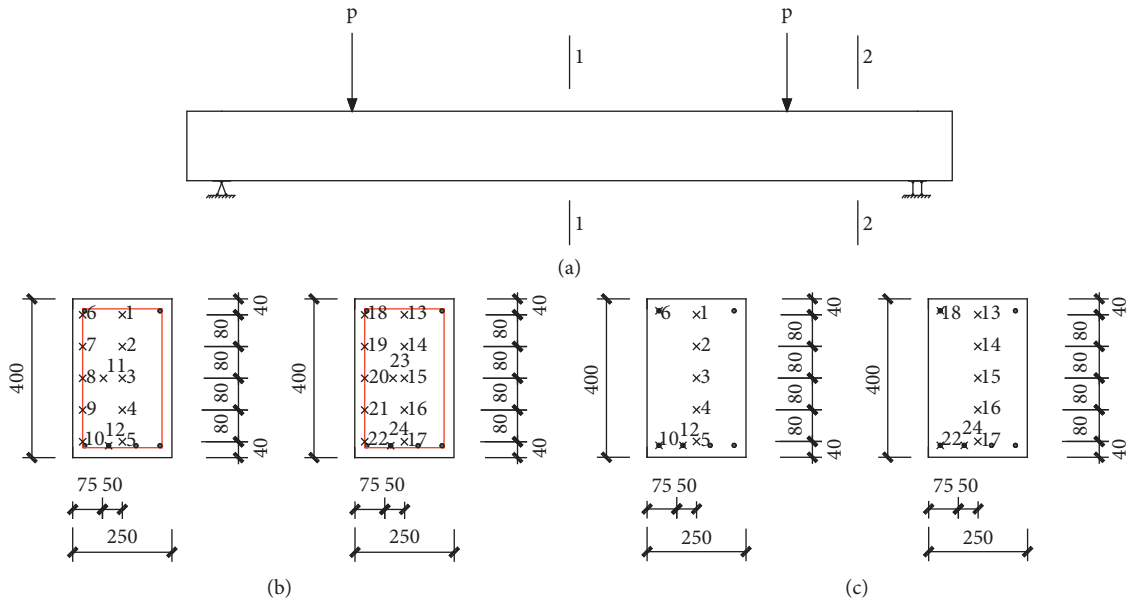


FIGURE 3: Location of thermocouples (dimensions in mm). (a) Elevation; (b) B2, B3, B4, and B5; (c) B6.

the failure mode and crack distribution, it can be seen from Figure 8(c) that the failure mode had the characteristic of the shear-bend failure when specimen B4 reached the fire resistance.

Specimen B5 peeled off part of the concrete skin under the coupling of fire and load, exposing the aggregate, and many vertical cracks with a maximum width of 2 mm appeared in the pure bending section, as shown in Figure 8(d).



FIGURE 4: The failure modes of B1. (a) Overall failure mode; (b) partial failure mode.

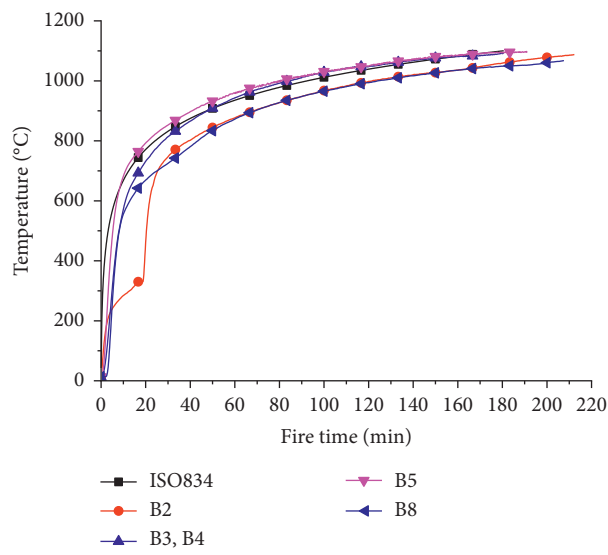


FIGURE 5: Measured time-temperature curve in the furnace.

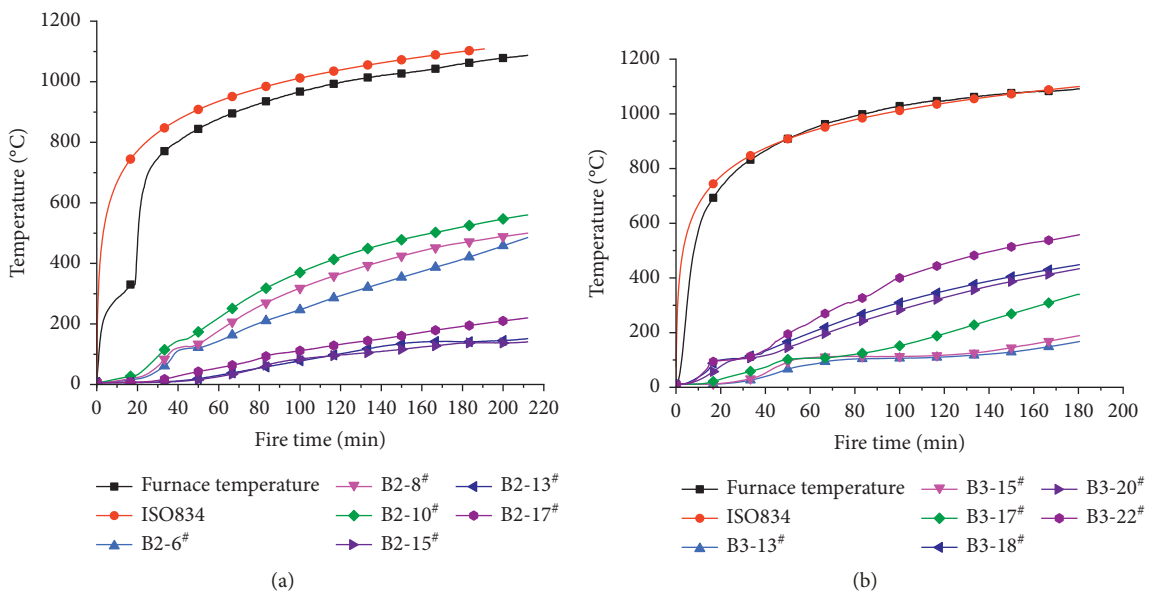


FIGURE 6: Continued.

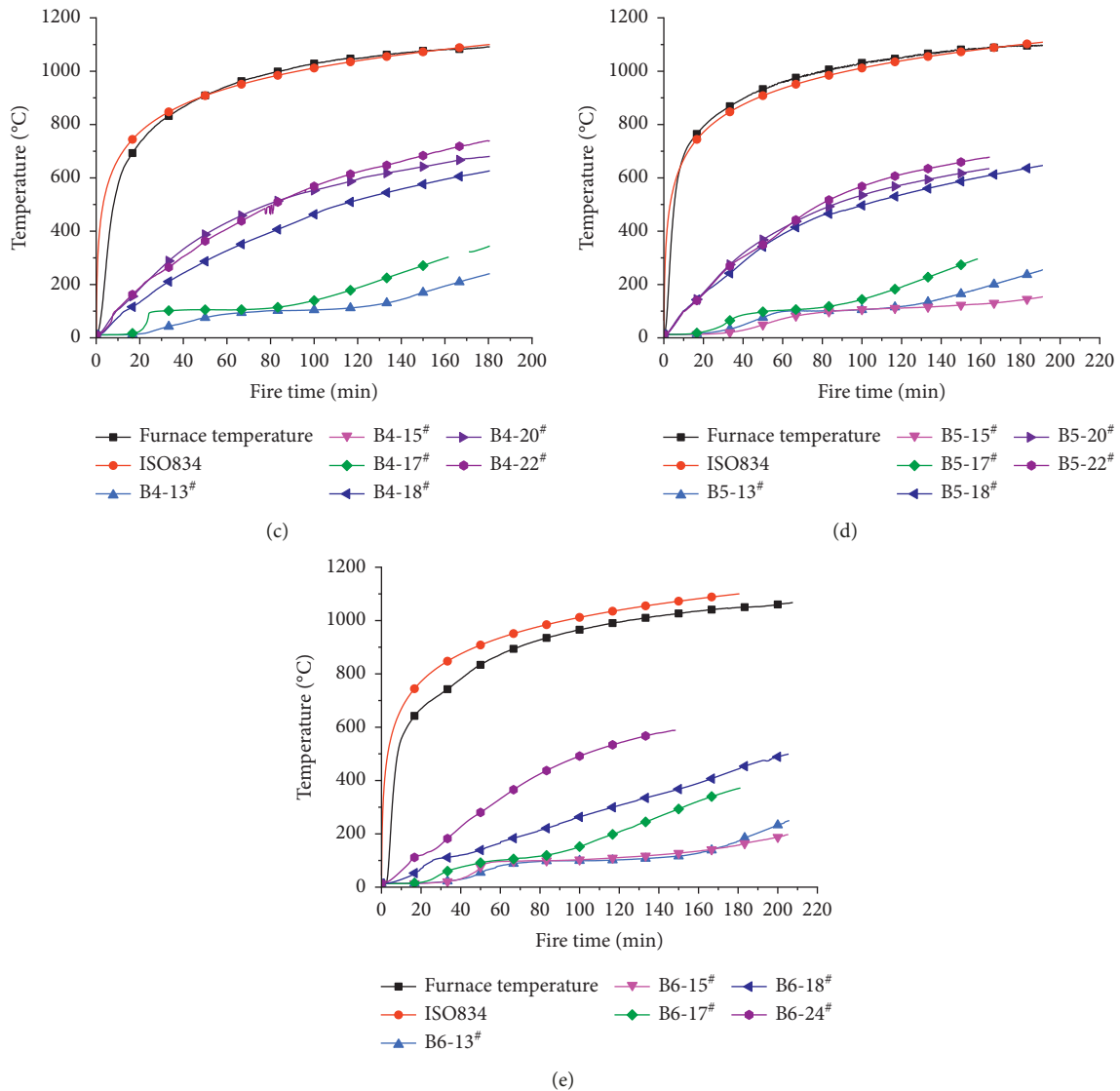


FIGURE 6: Measured temperature-time curves of the RC beam: (a) B2, (b) B3, (c) B4, (d) B5, and (e) B6.

TABLE 4: Fire resistances.

Specimen	$\rho_{sv}$ (%)	$\rho$ (%)	Failure time (min)
B2	0.27	1.96	192
B3	0.27	1.61	180
B4	0.27	1.47	171
B5	0.20	1.96	182
B6	0.00	1.96	198

The diagonal crack with the width of mostly 1 mm-2 mm emerged in the shear section. Observing the failure mode and crack distribution, specimen B5 had no obvious signs of shear failure under the thermal coupling effect, which had a tendency to shear-bend failure.

The concrete cover fell off nearly 3000 mm at the bottom of specimen B6, and the longitudinal steel were exposed, as illustrated in Figure 8(e). A large length of cracking occurred along the longitudinal direction of the beam, exposing the upper edge of the steel bar. The longitudinal splitting crack

should be caused by the thermal expansion and cracking expansion of the concrete without the restraint of the stirrup. Many vertical cracks appeared in the pure bend section, and the maximum width of the vertical cracks reached 6 mm, while the diagonal cracks in the shear-bending section were mostly 3 mm. Therefore, specimen B6 exhibited a shear-bend failure mode when it reached the fire resistance.

As can be seen in Table 4 and Figures 4 and 8, it is important to note that almost all beams, with the exception of B4, achieved 180 + minutes of failure time. This is pretty much comparable to an RC beam loaded primarily in flexure. The failure modes of beams at high temperature show very different shapes, comparing with the reference beams under room temperature. The change of failure mode shifting from shear failure at ambient temperature to shear-bend failure at high temperature may be caused by a combination effect of compression and shear, the concrete in shear-compression crushed accompanied with spalling of concrete cover, the strength degradation of concrete exposed

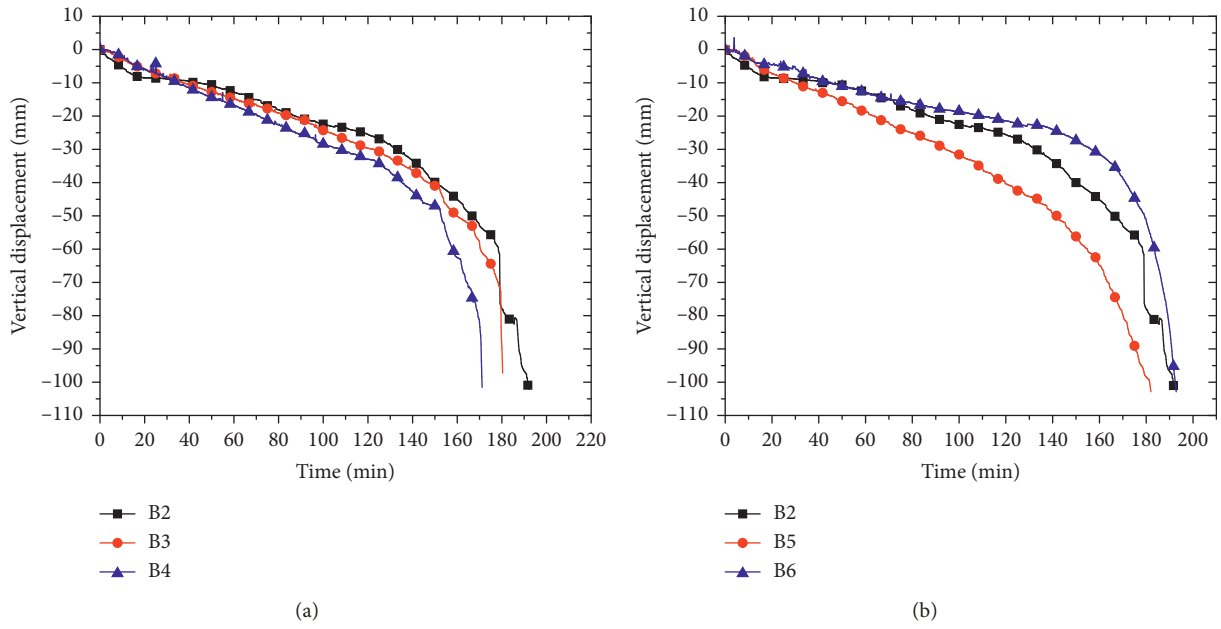


FIGURE 7: Measured deflection-time curve of the maximum displacement point: (a) B2, B3, and B4;(b) B2, B5, and B6.

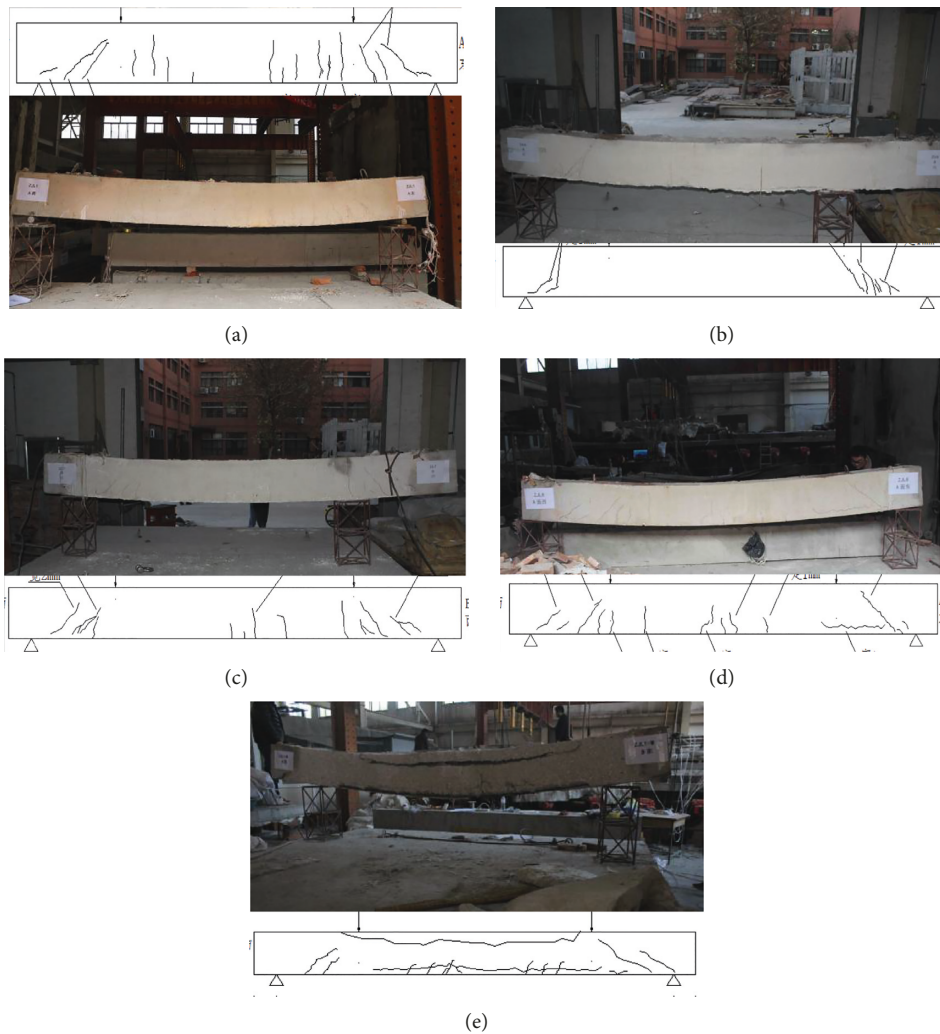


FIGURE 8: The failure modes of RC beams (dimensions in mm): (a) B2, (b) B3, (c) B4, (d) B5, and (e) B6.

to fire, thermal expansion cracking expansion, and so on. Therefore, according to the design principle of “strong-bending and weak shearing” at room temperature, the failure mode of the specimen may be shear-bend failure under the thermal coupling, and perhaps shear failure may not be a brittle failure mode under fire conditions.

## 5. Conclusions

To investigate the fire resistance of RC beams, six RC beams were tested with different longitudinal reinforcement ratio and stirrup ratio. The main outcomes can be summarized as follows:

- (1) According to the design principle of “strong bending and weak shearing,” the simple supported RC beam with stirrup reinforcement was the shear failure under room temperature, while the failure mode might be shear-bend failure at high temperature.
- (2) The greater the longitudinal reinforcement ratio, the longer the failure time of the specimen. It indicated that the pinning action of the longitudinal reinforcement could significantly improve the shear capacity of beams at high temperature.
- (3) When the applied load ratio was constant, the stirrup ratio had no obvious regular effect on the fire resistance of the RC beam under fire exposure, but the configuration of the stirrup could effectively reduce the brittle change of the vertical displacement when the beam entered the failure stage.

## Data Availability

All data included in this study are available upon request from the corresponding author.

## Conflicts of Interest

The authors declare no potential conflicts of interest with respect to the research, authorship, and/or publication of this article.

## Acknowledgments

This work was financially supported by the National Natural Science Foundation of China (51478254).

## References

- [1] Z. D. Lu, B. L. Zhu, and Y. H. Zhou, “Experimental study on fire response of simple supported reinforced concrete beams,” *China Civil Engineering Journal*, vol. 26, no. 3, pp. 47–54, 1993.
- [2] C. G. Fu, Y. Z. Wang, D. S. Yu et al., “Experimental study on bearing behavior of prestressed steel reinforced concrete simply supported beam under fire and vertical load,” *Journal of Disaster Prevention and Mitigation Engineering*, vol. 32, no. 1, pp. 1–7, 2012.
- [3] M. S. Khan, J. Prasad, and H. Abbas, “Shear strength of RC beams subjected to cyclic thermal loading,” *Construction and Building Materials*, vol. 24, no. 10, pp. 1869–1877, 2010.
- [4] A. Faris, N. Ali, S. Gordon, and A.-T. Abid, “Outcomes of a major research on fire resistance of concrete columns,” *Fire Safety Journal*, vol. 39, no. 6, pp. 433–445, 2004.
- [5] A. Ahmed and V. Kodur, “The experimental behavior of FRP-strengthened RC beams subjected to design fire exposure,” *Engineering Structures*, vol. 33, no. 7, pp. 2201–2211, 2011.
- [6] M. B. Dwaikat and V. K. R. Kodur, “Response of restrained concrete beams under design fire exposure,” *Journal of Structural Engineering*, vol. 135, no. 11, pp. 1408–1417, 2009.
- [7] E. Ryu, Y. Shin, and H. Kim, “Effect of loading and beam sizes on the structural behaviors of reinforced concrete beams under and after fire,” *International Journal of Concrete Structures and Materials*, vol. 12, no. 1, pp. 1–10, 2018.
- [8] B. Wu, W. Xiong, and B. Wen, “Thermal fields of cracked concrete members in fire,” *Fire Safety Journal*, vol. 66, pp. 15–24, 2014.
- [9] D. E. Christopher and J. Elin, “Reliability analysis of prestressed concrete beams exposed to fire,” *Engineering Structures*, vol. 43, pp. 69–77, 2012.
- [10] J. Kang, H. Yoon, W. Kim, V. Kodur, Y. Shin, and H. Kim, “Effect of wall thickness on thermal behaviors of RC walls under fire conditions,” *International Journal of Concrete Structures and Materials*, vol. 10, no. 3, pp. 19–31, 2016.
- [11] L. A. Gabriela, B. S. Augusto, P. C. R. Joao, and P. S. Valdir, “Behavior of thermally restrained RC beams in case of fire,” *Engineering Structures*, vol. 174, pp. 407–417, 2018.
- [12] C. G. Fu, Y. M. Song, A. K. Yin et al., “Experimental study on shear bearing capacity of reinforced concrete beams under thermodynamic coupling,” *Journal of Shandong Jianzhu University*, vol. 33, no. 5, pp. 1–10, 2018.
- [13] Z. Huang, I. W. Burgess, and R. J. Plank, “Non-linear structural modelling of a fire test subject to high restraint,” *Fire Safety Journal*, vol. 36, no. 8, pp. 795–814, 2001.
- [14] L.-H. Han, Z. Y.-Q. Zheng, and Z. Tao, “Fire performance of steel-reinforced concrete beam-column joints,” *Magazine of Concrete Research*, vol. 61, no. 7, pp. 499–518, 2009.
- [15] G. Y. Wang, L. H. Han, and H. X. Yu, “Fire performance of reinforced concrete beam-column plane joints,” *Engineering Mechanics*, vol. 27, no. 12, pp. 164–173, 2010.
- [16] Z. N. Yang, M. Y. Chen, X. G. Wang et al., “Research on shear behavior of reinforced concrete frame beams at high temperature,” *Journal of Guangxi University (Natural Science Edition)*, vol. 41, no. 4, pp. 1054–1060, 2016.
- [17] W. Y. Gao, J.-G. Dai, J. G. Teng, and G. M. Chen, “Finite element modeling of reinforced concrete beams exposed to fire,” *Engineering Structures*, vol. 52, no. 7, pp. 488–501, 2013.
- [18] X. Lin and Y. X. Zhang, “Nonlinear finite element analyses of steel/FRP-reinforced concrete beams in fire conditions,” *Composite Structures*, vol. 97, no. 3, pp. 277–285, 2013.
- [19] C. G. Fu, W. Liu, and W. Y. Kong, “The temperature field analysis of reinforced concrete beam based on heating and cooling whole curve,” *Journal of Shandong Jianzhu University*, vol. 30, no. 4, pp. 307–317, 2015.
- [20] L. G. Jia, Y. H. Wang, L. S. Wang et al., “Study on fire resistance of steel casted beam-concrete slab composite beams,” *Journal of Shenyang Jianzhu University (Natural Science)*, vol. 34, no. 5, pp. 769–776, 2018.
- [21] G. Bihina, B. Zhao, and A. Bouchair, “Behaviour of composite steel-concrete cellular beams in fire,” *Engineering Structures*, vol. 56, no. 6, pp. 2217–2228, 2013.

- [22] ISO- International Organization for Standardization, *ISO 834: Fire-Resistance Tests: Elements of Building Construction, Part 1.1: General Requirements for Fire Resistance Testing*, ISO-International Organization for Standardization, Geneva, Switzerland, 1990.
- [23] Standards Press of China, *National Standard of the People's Republic of China, Fire-resistance Tests-element of Building Construction-Part 1: General Requirements (GB/T9978.1-2008)*, Standards Press of China, Beijing, China, 2009.
- [24] China Architecture and Building Press, *GB 50010-2010, Code for Design of Concrete Structures*, China Architecture and Building Press, Beijing, China, 2015.

